DOI: 10.1002/ejic.201000446

Construction of a Series of 1D and 2D Inorganic–Organic Hybrid Coordination Polymers Based on 1,1′-Bis(propionic acid)-2,2′-biimidazole

Rui-Li Sang[a] and Li Xu*[a]

Keywords: Organic-inorganic hybrid composites / Coordination polymers / Polymers / N ligands / Cadmium / Zinc

The substitution reactions of cadmium or zinc nitrate and the new multifunctional ligand Pra_2biim^{2-} [Pra_2biim = 1,1′-bis(propionic acid)-2,2′-biimidazole] produce a series of coordination polymers with d^{10} metal centers, namely, 1D $[Cd(HPra_2biim)(H_2O)Cl]_n \cdot nH_2O$ (**1**), 1D $[Cd_2(Pra_2biim)(H_2O)_4(NO_3)_2]_n$ (**2**), and 2D $[Zn(HPra_2biim)Cl]_n$ (**3**) in acidic aqueous solutions. The presence of a strong inorganic acid, such as HCl, lead to the protonation of Pra_2biim^{2-} as observed in polymers **1** and **3**. Compounds **1** and **3** contain the doubly *N*,*N*′-biim-bridged $[M_2(\mu_2\text{-}N,N'\text{-biim})_2]$ and compound **2** the singly bridged $[M_2(\mu_2\text{-}N,N'\text{-biim})]$ as secondary building blocks that are interconnected by the propionate arms into 1D chains in **1** and **2**, and into a 2D layer in **3**. These d^{10} metal polymers exhibit luminescent emissions that are sensitive to the coordination geometry of the metal centers.

Introduction

The design and synthesis of functional coordination polymers built of metal ions and organic linkers have received considerable attention in recent years due to the intriguing structural diversities and potential applications.[1–8] Although most coordination polymers contain more than one organic linker, single-linker-based coordination polymers have advantages in aspects such as stability and have less elements of difficulty and hence greater predictability. An ideal single organic linker should contain a pair of donor atoms bridging metal ions together and additional arms capable of interconnecting the resulting metal cluster units into extended architectures. The compound 2,2′-biimidazole (H_2biim) has been widely used as a biomimetic ligand in bioinorganic chemistry,[9,10] a bridging ligand in oligometallic chemistry for catalysis[11,12] and antitumour drugs,[13,14] and as a building blocks in supramolecular frameworks.[15–18] Recently, it has been shown that *N*-substituted biimidazoles, such as *N*,*N*′-dimethylated derivatives of biimidazole (Me_2biim), prefer a bridging rather than a chelating coordination mode because of the noncoplanarity of the two imidazole rings as indicated by the large dihedral angle (67–89°), which is believed to be caused by repulsion between the substituents.[19,20] Hence, it can serve as a good bridging ligand to link metal ions together. Meanwhile, polycarboxylic groups have proven to be the most successful linkers in the construction of metal–organic frameworks (MOFs) because of their structural rigidity, chemical stability, and strong coordinating ability.[21,22] With these two factors in mind, the multifunctional ligand Pra_2biim^{2-} [1,1′-bis(propionic acid)-2,2′-biimidazole],[23] as shown in Scheme 1, was selected for the following reasons: (i) the cooperative coordination of the nitrogen atoms and propionate arms is expected to exhibit varied coordinating modes; and (ii) the flexibility and chirality induced by the free rotation around the central C–C bond and two propionate arms are expected to display the versatile coordination chemistry of this new multifunctional ligand (Scheme 1). In this contribution, we wish to report on the synthesis, X-ray structural studies, and photoluminescence of the protonated ligand H_2Pra_2biim (**L**) and three new d^{10}-metal coordination polymers, $[Cd(HPra_2biim)(H_2O)Cl]_n \cdot nH_2O$ (**1**), $[Cd_2(Pra_2biim)(H_2O)_4(NO_3)_2]_n$ (**2**), and $[Zn(HPra_2biim)Cl]_n$ (**3**).

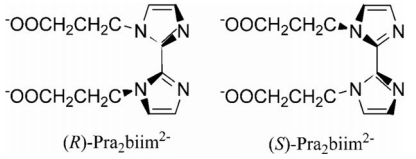

Scheme 1. The configuration of the Pra_2biim^{2-} ligand.

Results and Discussion

Syntheses

The syntheses of polymers **1**–**3** are summarized in Scheme 2. The related displacement reactions of the $[M(Me_2biim)]$ (M = Zn, Cd, Cu, Cr) systems has been shown to form singly, doubly, triply, and even quadruply bridged species because of the remarkable repulsion be-

[a] State Key Laboratory of Structural Chemistry, Fujian Institute of Research on the Structure of Matter, Chinese Academy of Science,
Fuzhou, Fujian 350002, P. R. China
Fax: +86-591-83705045
E-mail: xli@fjirsm.ac.cn

tween the methyl substituents.[19,20] As shown in Scheme 2, the use of the *N*-carboxylated derivative Pra_2biim^{2-} instead of Me_2biim affords polymeric products rather than discrete ones because of coordination of the carboxylic arms. This can yield insoluble reaction products and often acids are needed to dissolve the precipitates for recrystallization. The polymerization depends on the extent to which the substitution reactions proceed; this is closely related to the reaction conditions, including the nature of the acids and the temperature. In the presence of an inorganic acid of considerable coordinating ability, such as HCl, one of the carboxylate arms is protonated, accompanied with the metal coordination of Cl, leading to the incomplete substitution of coordinated water and Cl as observed in the 1D $[Cd(HPra_2biim)(H_2O)Cl]_n \cdot nH_2O$ (**1**). The displacement reactions are also metal-dependent. The use of Zn^{2+} of lower coordination number in place of Cd^{2+} gives the complete replacement of the coordinating water by the carboxylic group, leading to the 2D polymer $[Zn(HPra_2biim)Cl]_n$ (**3**). The addition of an organic acid, such as acetic acid, does not result in the protonation of the carboxylic groups as indicated by the formation of the 1D $[Cd_2(Pra_2biim)(H_2O)_4(NO_3)_2]_n$ (**2**), but the chelating coordination of the nitrate anions to the metal ion reduces the connecting nodes of the metal ion and disfavors the complete displacement of water, leading to the lower dimensionality as will be described below (see Scheme 3).

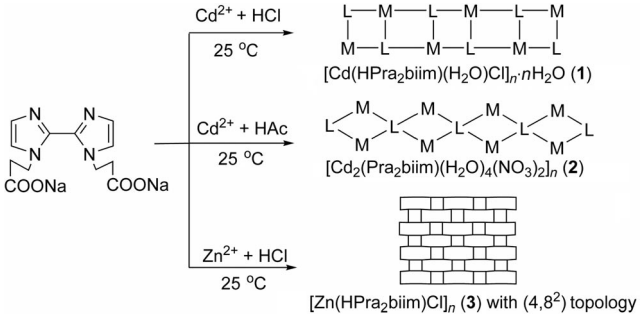

Scheme 2. The syntheses of compounds **1**–**3**.

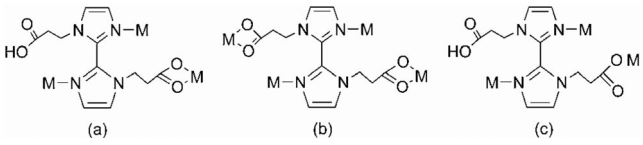

Scheme 3. The coordinating modes of Pra_2biim^{2-} observed in **1**–**3**.

X-ray Analyses

H_2Pra_2biim (L)

The numbering scheme and atom connectivity for H_2Pra_2biim, which contains a crystallographic center of inversion, is shown in Figure 1. The two imidazole rings are coplanar with the two carboxylic arms *trans* to each other to achieve the optimum environment for resonance delocalization and the least repulsion between the substituents. Most importantly, such a planar *anti* conformation favors the formation of the $CO_2H\cdots N$ hydrogen bonds [O1···N2A 2.7631(17) Å] (Table 1), which leads to a (4,4) 2D supramolecular sheet in the *ac* plane with the H_2Pra_2biim ligand acting as four-connected node as shown in Figure 2.

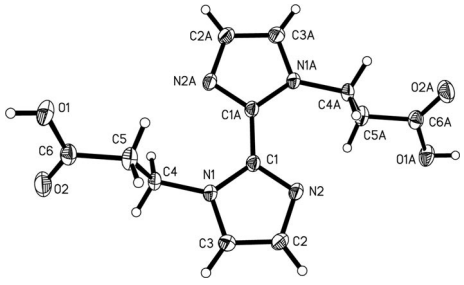

Figure 1. Molecular structure of H_2Pra_2biim.

Table 1. Hydrogen bond lengths [Å] and angles [°] for **L** and compounds **1**–**3**.

D–H···A	*d*(D–H)	*d*(H···A)	*d*(D···A)	∠(DHA)	Symmetry code
L					
O(1)–H(1)···N(2)	0.82	1.9	2.7631(17)	173.8	$x + 1, -y + 1/2, z + 1/2$
Complex **1**					
O(1 W)–H(1WB)···Cl(1)	0.85	2.48	3.230(5)	147.0	$-x + 1, -y + 1, -z + 1$
O(1 W)–H(1WA)···O(4)	0.85	1.89	2.708(6)	160.9	$x, y–1, z$
O(5)–H(5D)···O(1 W)	0.85	2.51	3.031(6)	120.3	$-x + 1, -y + 1, -z + 1$
O(5)–H(5D)···O(2)	0.85	2.15	2.889(6)	145.9	$-x + 2, -y + 1, -z + 1$
O(5)–H(5C)···O(3)	0.85	1.83	2.673(5)	169.5	$-x + 1, -y + 1, -z + 1$
O(1)–H(1)···O(1 W)	0.82	1.75	2.549(6)	162.9	$x + 1, y, z$
Complex **2**					
O(7)–H(7A)···O(1)	0.90	1.81	2.706(2)	176.6	$-x + 1, y – 1, -z + 1/2$
O(7)–H(7B)···O(4)	0.87	2.17	3.031(3)	170.0	$-x + 1, y, -z + 1/2$
O(6)–H(6A)···O(2)	0.87	1.93	2.778(2)	165.1	$-x + 1, -y, -z + 1$
O(6)–H(6B)···O(3)	0.86	1.96	2.824(3)	174.7	$-x + 1/2, y + 1/2, -z + 1/2$
Complex **3**					
O(2)–H(2)···O(4)	0.82	1.83	2.638(3)	169.6	$-x + 1, -y + 1, -z + 1$

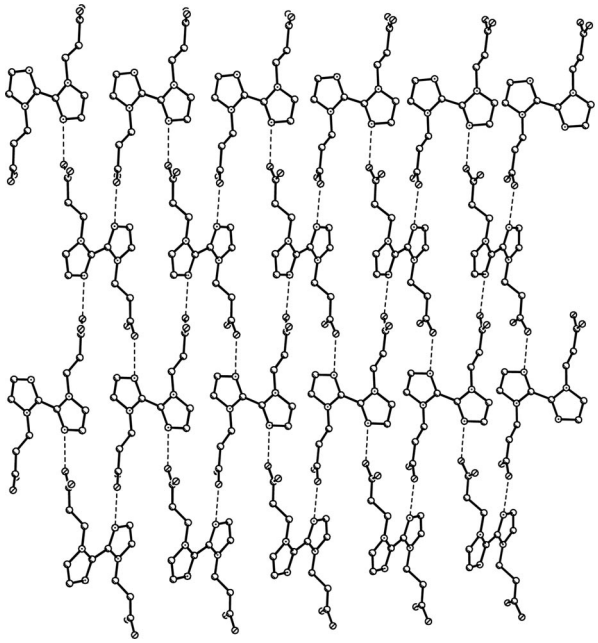

Figure 2. A single (4,4) 2D hydrogen-bonded sheet in **L**.

[Cd(HPra$_2$biim)(H2O)Cl]$_n$·nH2O (1)

As in the case of $[Zn_2(\mu_2\text{-}Me_2biim)_2]^{4+}$,[19] the Cd ions are centrosymmetrically doubly-bridged by the nitrogen atoms to form the basic $[Cd_2(\mu_2\text{-}Hpra_2biim)_2]^{2+}$ ion (Figure 3, a) with a dihedral angle of the two imidazole rings of 72.8°. Each Cd^{2+} ion has a distorted octahedral geometry with the equatorial positions occupied by a nitrogen atom of the imidazole moiety, a chlorine ion, and the chelating carboxylic oxygen atoms; the apical positions are occupied by the second nitrogen atom of the imidazole group and one coordinating water molecule. In contrast to the case of the coordinated carboxylic arm [C(12)–O(3) 1.262(6), C(12)–O(4) 1.258(6) Å], the marked difference between C(6)–O(1) [1.289(6) Å] and C(6)–O(2) [1.201(6) Å] of the free carboxylic group is clearly indicative of protonation. The dinuclear units are interconnected by the chelating carboxylic arm and form a 1D ladder-like chain running along the *a* axis (Figure 3, b and Scheme 1) with the coordinating mode indicated in Scheme 3 (a) (the pitch is 9.053 Å). The hydrogen bonds between the coordinating water molecule (O5) and the carboxylate oxygen atoms [O(5)···O(2) 2.889(6); O(5)···O(3) 2.673(5) Å] and the π-π stacking interactions (face-to-face distance, ca. 3.90 Å) link the infinite chain into a 2D supramolecular layer (Figure 3, b) in the *ac* plane. The strong hydrogen bonds between the lattice water molecule (O5) and the carboxylic groups [O1–H$^+$···O1W 2.549(6); O1W–H···O4 2.708(6) Å] interconnect the layers into 3D supramolecular frameworks that are further stabilized by hydrogen bonds between the lattice water molecule (O5) and the chlorine atoms or coordinated water molecules [O1W–H···Cl1 = 3.230(5); O1W–H···O5 3.031(6) Å] (Table 1 and Figure S1 in the Supporting Information).

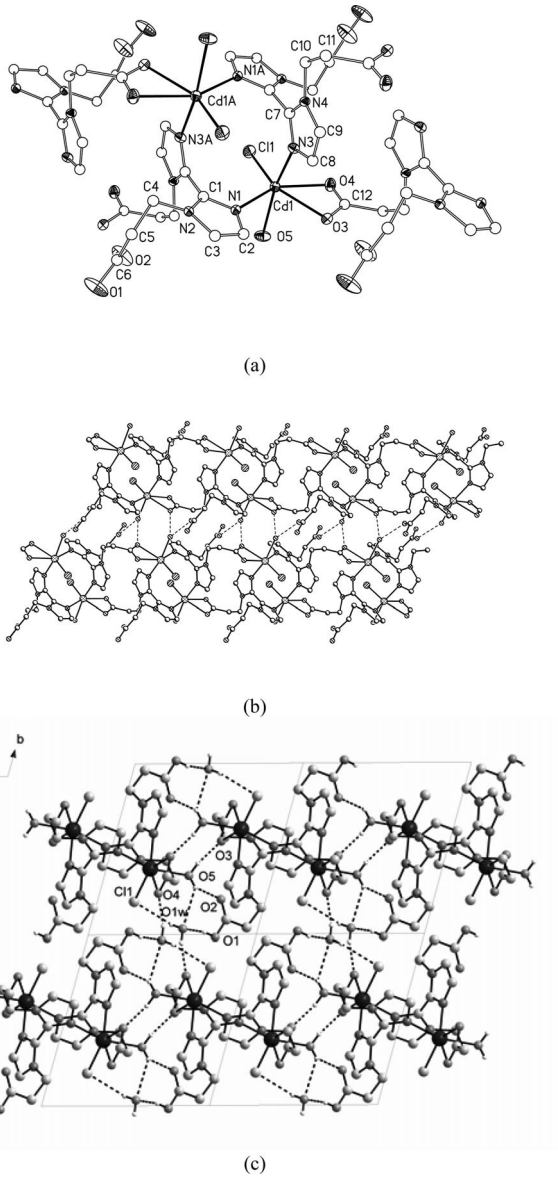

Figure 3. (a) The binuclear structure and coordination environment of the Cd^{2+}ions in **1**; (b) the 1D ladder-like structure and hydrogen bonds between adjacent chains in **1**; and (c) the 3D supramolecular network.

[Cd$_2$(Pra$_2$biim)(H$_2$O)$_4$(NO$_3$)$_2$]$_n$ (2)

As shown in part a of Figure 4, the Cd atom has a distorted pentagonal bipyramidal geometry with the equatorial sites occupied by the chelating nitrate and carboxylate groups, and the nitrogen atoms of the imidazole moiety; the apical positions are occupied by water molecules. The singly *N*,*N*′-bridged dinuclear structure has been observed in **2** as a consequence of the coordination of the nitrate group as illustrated in Figure 4 (a). The ligand has a coordinating mode (Scheme 2, b) similar to that found in $[Cd(Pra_2biim)(H_2O)]_n\cdot 2nH_2O$[23] but the dihedral angle in **2** (125.7°) is significantly larger than that in $[Cd(Pra_2biim)(H_2O)]_n\cdot 2nH_2O$ (62.7°). The dinuclear units are interconnected by the two chelating propionate arms into a zigzagged infinite chain along the [101] direction with a pitch of 13.356 Å

(Figure 4, b and Scheme 1). The chain is further stabilized by the weak hydrogen bonds between the coordinating water molecule (O7) and the nitrate oxygen [O(7)···O(4) 3.031(3) Å] (Figure 4, a). The adjacent ribbons are linked by the hydrogen bonds between O7 and propionate oxygen (O1) [O(7)···O(1) 2.706(2) Å] into 2D sheets (Figure 4, b). The hydrogen bonds between the coordinated water molecule (O6) and propionate oxygen atoms [O(6)···O(2) 2.778(2); O(6)···O(3) 2.824(3) Å] link the adjacent layers into a 3D supramolecular framework (Figure 4, c and Table 1).

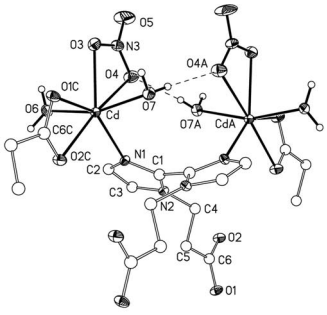

(a)

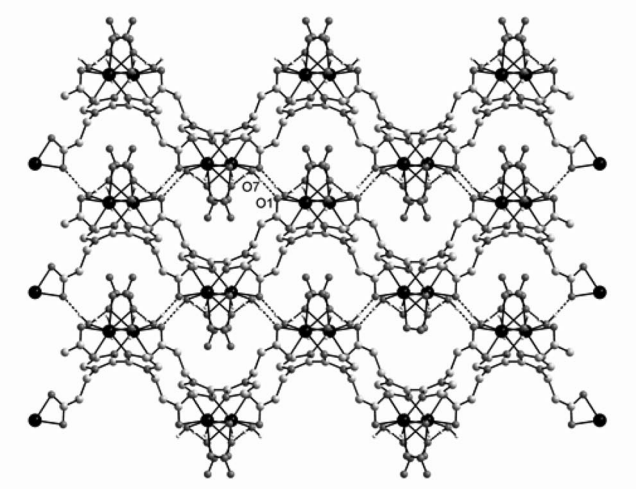

(b)

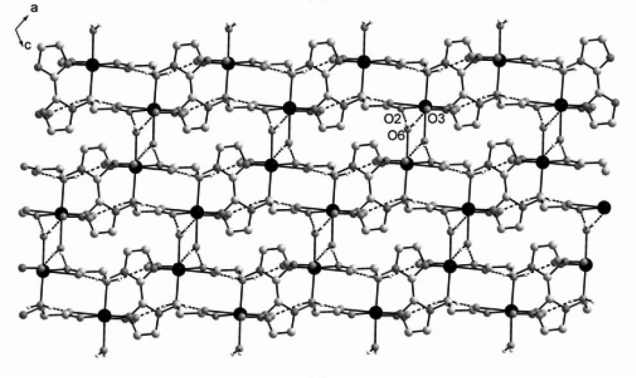

(c)

Figure 4. (a) View of the binuclear structure of **2** [O(7)···O(4) 3.031(3) Å]; (b) the zigzag chains interconnected by complementary CO_2···HOH hydrogen bonds into a 2D layer [O(7)···O(1) 2.706(2) Å]; (c) the 3D supramolecular framework formed through hydrogen bonds between the coordinating water O6 and propionate group [O(6)···O(2) 2.778(2); O(6)···O(3) 2.824(3) Å].

[Zn(HPra$_2$biim)Cl]$_n$ (3)

Polymer **3** features the doubly *N*,*N*′-bridged $[Zn_2(\mu_2\text{-}HPra_2biim)_2]^{2+}$ unit reminiscent of $[Zn_2(\mu_2\text{-}Me_2biim)_2]^{4+}$[23] (Figure 5, a). Both have a centrosymmetric structure with

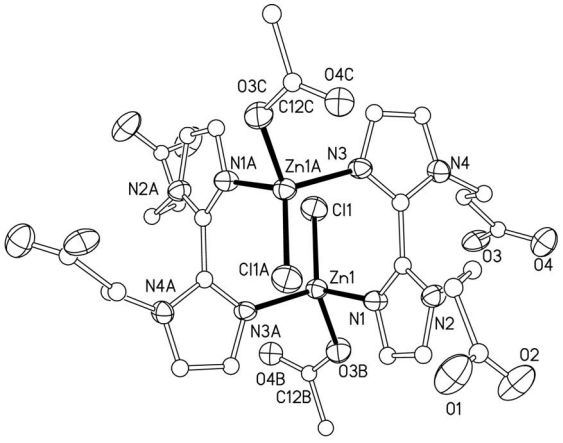

(a)

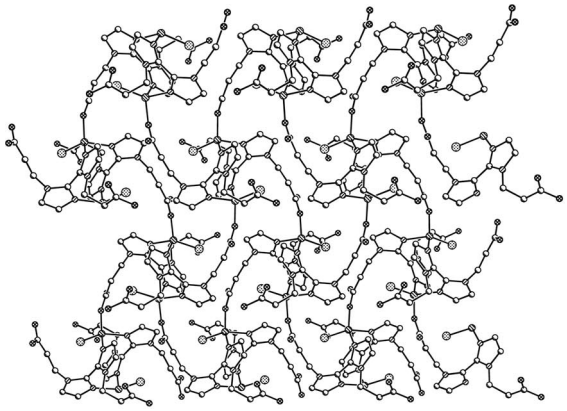

(b)

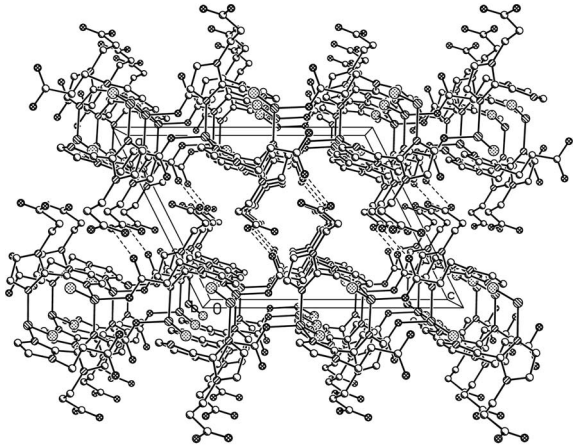

(c)

Figure 5. (a) View of the $[Zn_2(\mu_2\text{-}HPra_2biim)_2]^{2+}$ SBU of **3**; (b) the 2D sheet structure of **3**; and (c) the 3D supramolecular network of **3** viewed along the *b* axis.

tetrahedrally coordinated Zn ions. The dihedral angle of the imidazole rings in **3** (85.8°) is close to that in $[Zn_2Cl_4(\mu_2\text{-}Me_2biim)_2]$ (85°).[23] The Zn–Cl [2.1930(8) Å] and Zn–N [2.043(2), 2.023(2) Å] bond lengths are not significantly different from those in $[Zn_2Cl_4(\mu_2\text{-}Me_2biim)_2]$, which are slightly longer than the Zn–O bond [1.9373(19) Å] in **3**. The structural evolution from the discrete $[Zn_2Cl_4(\mu_2\text{-}Me_2biim)_2]$ complex to the present 2D $[Zn(HPra_2biim)Cl]_n$ polymer occurs as a consequence of the substitution of one Cl^- ion in $[Zn_2Cl_4(\mu_2\text{-}Me_2biim)_2]$ with one deprotonated propionate arm in **3**. Similar to **1**, the protonated carboxylic group features significant differences in the C–O bond lengths [C(6)–O(1) 1.317(4); C(6)–O(2) 1.203(3) Å]. Unlike **1**, the deprotonated propionate arm acts as a monodentate ligand, as illustrated in Scheme 3 (c) and presumably caused by the lower coordination number of Zn^{2+}, to interconnect the $[Zn_2(\mu_2\text{-}N,N'\text{-}biim)_2]$ secondary building blocks (SBUs) into a 2D-layered structure in the *bc* plane (Figure 5, b). The sheet structure of **3** has a $4{\cdot}8^2$ topology (Scheme 1) with both the Zn^{2+} ion and the Pra_2biim^{2-} ligand acting as four-connected nodes. The adjacent layers interact with each other through strong hydrogen bonding interactions between the protonated and deprotonated propionate arms [O2···O4 2.638(3) Å] yielding a 3D supramolecular framework (Figure 5, c and Table 1).

Fluorescent Properties

Metal complexes are promising luminescent materials for various applications, such as light-emitting materials, owing to their ability to enhance, shift, and quench luminescent emission of organic ligands by metal coordination. Complexes consisting of d^{10} metals have been shown to exhibit interesting photoluminescent properties.[24–26] The fluorescent spectra of the Na_2Pra_2biim ligand, and complexes **1**–**3** in the solid state at room temperature are shown in Figure 6. Polymers **1** and **3** exhibit violet photoluminescent emission [365.5 nm (λ_{ex} = 290 nm) for **1**, and 367.5 nm (λ_{ex} = 292 nm) for **3**] similar to that of Na_2Pra_2biim [337 nm (λ_{ex} = 280 nm)], which can be attributed to the ligand-centered emission. Interestingly, compound **2** shows greenish-blue photoluminescence with an emission maximum at 502 nm upon excitation at 372 nm. The spectrum of **2** has a considerably longer emission maximum and greater middle-width than that of the free ligand, and is presumably assigned to metal–ligand charge transfer (MLCT). This is believed to be caused by the coordination of the Cd^{2+} ion of **2** to one chelating nitrate anion and two water molecules that are hydrogen bonded to the neighboring nitrate moiety. The quenching of ligand emission by water molecules that interact with neighboring groups has been reported previously.[27]

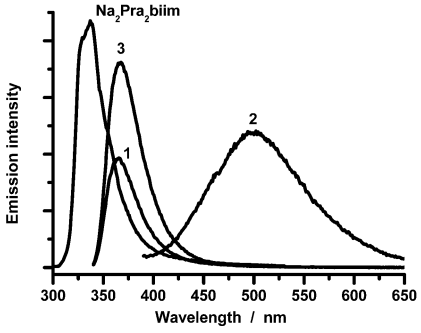

Figure 6. Luminescent emission spectra of Na_2Pra_2biim, **1**–**3**.

Conclusion

In summary, the three novel coordination polymers **1**–**3** constructed from d^{10} metal ions and the newly designed Pra_2biim^{2-} ligand with three different coordinating modes have been obtained and characterized by X-ray crystallography and luminescence spectroscopy. This has revealed an efficient route to single-linker-based coordination polymers by functionalizing known organic bridging ligands. The use of an inorganic acid, such as HCl, lead to the protonation of one of the carboxylic arms of Pra_2biim^{2-} in some cases. These d^{10}–Pra_2biim^{2-} polymers feature the binuclear $[M_2(\mu_n\text{-}N,N'\text{-}biim)_n]$ (n = 1, 2) SBUs that are interconnected by carboxylic arms into 1D ladder (**1**) or zigzagged chains (**2**) and 2D layers (**3**). The photoluminescent properties of $[M(Pra_2biim)]$ coordination polymers have been found to be sensitive to the coordination geometry of metal centers.

Experimental Section

General Remarks: 1,1′-Bis(ethylpropionato)-2,2′-biimidazole ($Epra_2biim$) was synthesized in accordance with a published procedure.[28] Na_2Pra_2biim was prepared by hydrolyzing $Epra_2biim$ and was characterized by IR and ^1H NMR spectroscopy. All other reagents and solvents employed were commercially available and used as received without further purification. The C, H, and N microanalyses were carried out with a Vario EL III elemental analyzer. IR spectra were recorded on a Magna 750 FTIR spectrometer photometer as KBr pellets. Fluorescent spectra were measured with an Edinburgh FLS920 analytical instrument.

H_2Pra_2biim (L): An aqueous solution of Na_2Pra_2biim (0.5 mmol, 10 mL) was acidified with 1 M HCl to pH 2.7 and allowed to stand at r.t. for several hours to yield colorless crystals of the title compound. The crystals were collected by filtration, washed with ethanol, and dried. $C_{12}H_{14}N_4O_4$ (278.27): calcd. C 51.80, H 5.07, N 20.13; found C 51.67, H 5.19, N 20.07.

$[Cd(HPra_2biim)(H_2O)Cl]_n{\cdot}nH_2O$ (1): Na_2Pra_2biim (0.20 mmol, 0.064 g) in water (3 mL) was slowly added to an aqueous solution (3 mL) of $Cd(NO_3)_2{\cdot}4H_2O$ (0.2 mmol, 0.062 g) resulting in immediate precipitation. The resulting mixture was adjusted to pH ≈ 3 with dilute HCl, dissolving the precipitate, and stirred for 1 h. The solution was filtered and the filtrate was left in air to evaporate. Colorless crystals were obtained after a few days. The product was

collected by filtration, washed with ethanol and dried in air. Yield 0.052 g, 56% (based on $Cd(NO_3)_2{\cdot}4H_2O$). $C_{12}H_{17}CdClN_4O_6$ (461.16): calcd. C 31.25, H 3.72, N 12.15; found C 30.69, H 3.60, N 12.10. IR (KBr): $\tilde{\nu}$ = 3545 (s), 3395 (s), 3131 (s), 2939 (w), 2752 (w), 2533 (w), 1717 (s), 1706 (s), 1566 (vs), 1521 (w), 1474 (m), 1435 (m), 1425 (m), 1391 (m), 1366 (w), 1330 (w), 1283 (s), 1272 (s), 1233 (s), 1149 (s), 986 (w), 949 (w), 896 (w), 771 (m), 757 (m), 735 (m), 724 (s), 631 (w) cm^{-1}.

$[Cd_2(Pra_2biim)(H_2O)_4(NO_3)_2]_n$ (2): Na_2Pra_2biim (0.20 mmol, 0.064 g) in ethanol (2 mL) was slowly added to a DMF solution (3 mL) of $Cd(NO_3)_2{\cdot}4H_2O$ (0.20 mmol, 0.062 g) resulting in immediate precipitation. The resulting mixture was adjusted to pH ≈ 3.5 with CH_3COOH and stirred at 80 °C for 1 h. The solution was filtered and the filtrate was left in air to evaporate. Colorless crystals were obtained after a few months. The product was collected by filtration, washed with ethanol and dried in air. Yield 0.024 g, 34% [based $Cd(NO_3)_2{\cdot}4H_2O$]. $C_{12}H_{20}Cd_2N_6O_{14}$ (697.14): calcd. C 20.67, H 2.89, N 12.05; found C 20.89, H 2.79, N 12.05. IR (KBr): $\tilde{\nu}$ = 3520 (s), 3400 (s), 3145 (s), 3003 (m), 1633 (w), 1547 (vs), 1468 (m), 1446 (vs), 1435 (vs), 1384 (vs), 1293 (vs), 1265 (s), 1148 (m), 1033 (w), 1025 (w), 962 (w), 643 (w), 834 (w), 817 (w), 771 (w), 726 (m), 686 (m) cm^{-1}.

$[Zn(HPra_2biim)Cl]_n$ (3): The procedure was the same as that for **1** using $Zn(NO)_3{\cdot}6H_2O$ (0.2 mmol, 0.060g) Yield 0.045 g, 59% [based $Zn(NO)_3{\cdot}6H_2O$]. $C_{12}H_{13}ClN_4O_4Zn$ (378.10): calcd. C 38.12, H 3.47, N 14.82; found C 37.99, H 3.53, N 14.69. IR (KBr): $\tilde{\nu}$ = 3453 (m), 3175 (m), 3151 (m), 3130 (m), 3020 (m), 2673 (w), 2586 (m), 1711 (vs), 1535 (w), 1486 (m), 1468 (s), 1443 (s), 1395 (s), 1384 (m), 1350 (w), 1287 (s), 1273 (m), 1250 (w), 1219 (w), 1152 (s), 1144 (s), 1059 (w), 967 (m), 955 (m), 774 (m), 738 (m), 728 (m) cm^{-1}.

Table 2. Crystallographic data for **L** and compounds **1**–**3**.

Compound	**L**	**1**	**2**	**3**
Molecular formula	$C_{12}H_{14}N_4O_4$	$C_{12}H_{17}CdClN_4O_6$	$C_6H_{10}CdN_3O_7$	$C_{12}H_{13}ClN_4O_4Zn$
Formula weight	278.27	461.16	348.57	378.10
Space group	$P2_1/c$ (No. 14)	$P\bar{1}$ (No. 2)	$C2/c$ (No.15)	$P2_1/c$ (No.14)
a [Å]	8.553(2)	9.0525(17)	18.408(17)	11.994(3)
b [Å]	6.2267(11)	10.041(2)	8.665(3)	9.112(2)
c [Å]	11.774(4)	10.068(2)	14.682(12)	15.451(3)
α [°]		103.330(8)		
β [°]	102.791(19)	109.713(6)	115.396	116.703(15)
γ [°]		93.728(4)		
Volume [Å^3]	611.5(3)	828.1(3)	2116(3)	1508.5(6)
Z	2	2	8	4
$d_{calcd.}$ [g/cm^3]	1.511	1.850	2.189	1.665
μ [mm^{-1}]	0.116	1.517	2.096	1.828
Goodness of fit	1.084	1.054	1.034	1.095
R_1 [$I > 2\sigma(I)$]	0.0411	0.0511	0.0188	0.0367
$wR2$ [$I > 2\sigma(I)$]	0.1143	0.0789	0.0465	0.0881
R_1 (all data)	0.0456	0.0730	0.0201	0.0477
wR_2 (all data)	0.1185	0.0902	0.0473	0.0938

Table 3. Selected bond lengths [Å] and angles [°] for compounds **1**–**3**.

Complex **1**					
Cd(1)–N(1)	2.314(4)	Cd(1)–N(3)	2.341(4)	Cd(1)–O(5)	2.353(3)
Cd(1)–Cl(1)	2.4632(14)	Cd(1)–O(4)	2.421(4)	Cd(1)–O(3)	2.426(3)
N(1)–Cd(1)–N(3)	86.34(14)	N(1)–Cd(1)–O(5)	84.06(13)	N(3)–Cd(1)–O(5)	162.08(13)
N(1)–Cd(1)–O(4)	151.35(13)	N(3)–Cd(1)–O(4)	91.06(13)	O(5)–Cd(1)–O(4)	90.15(13)
N(1)–Cd(1)–O(3)	97.88(13)	N(3)–Cd(1)–O(3)	81.63(13)	O(5)–Cd(1)–O(3)	84.73(13)
O(5)–Cd(1)–Cl(1)	91.80(10)	O(4)–Cd(1)–Cl(1)	93.53(10)	O(3)–Cd(1)–Cl(1)	146.80(9)
Complex **2**					
Cd–N(1)	2.2763(18)	Cd–O(1) #1	2.362(2)	Cd–O(2) #1	2.3729(17)
Cd–O(3)	2.4239(19)	Cd–O(4)	2.559(2)	Cd–O(7)	2.298(2)
Cd–O(6)	2.307(2)				
N(1)–Cd–O(7)	96.95(8)	N(1)–Cd–O(6)	92.94(8)	N(1)–Cd–O(1)#1	143.43(6)
N(1)–Cd–O(3)	130.17(6)	N(1)–Cd–O(4)	79.47(7)	O(6)–Cd–O(1)#1	93.91(10)
O(7)–Cd–O(6)	162.22(6)	O(7)–Cd–O(1)#1	86.93(9)	O(6)–Cd–O(2)#1	90.01(8)
O(7)–Cd–O(3)	82.19(6)	O(1)#1–Cd–O(3)	86.40(5)	O(7)–Cd–O(4)	82.73(9)
O(6)–Cd–O(3)	80.14(6)	O(2)#1–Cd–O(3)	139.48(6)	O(6)–Cd–O(4)	84.60(9)
O(3)–Cd–O(4)	50.87(5)	O(7)–Cd–O(2)#1	104.83(8)	O(1)#1–Cd–O(4)	136.95(6)
N(1)–Cd–O(2)#1	89.22(7)	O(1)#1–Cd–O(2)#1	54.93(6)	O(2)#1–Cd–O(4)	167.17(5)
Complex **3**					
Zn(1)–N(1)	2.043(2)	Zn(1)–N(3)#2	2.023(2)	Zn(1)–O(3)#1	1.9373(19)
Zn(1)–Cl(1)	2.1930(8)				
O(3)#1–Zn(1)–N(1)	94.36(8)	N(3)#2–Zn(1)–N(1)	102.58(8)	O(3)#1–Zn(1)–Cl(1)	121.88(6)
O(3)#1–Zn(1)–N(3)#2	105.81(8)	N(1)–Zn(1)–Cl(1)	115.71(6)	N(3)#2–Zn(1)–Cl(1)	113.47(6)

[a] For **2**: #1: $x - 1/2$, $-y + 1/2$, $z - 1/2$; for **3**: #1: $-x + 2$, $y - 1/2$, $-z + 3/2$, #2: $-x + 2$, $-y + 1$, $-z + 1$.

X-ray Crystallographic Studies: Suitable single crystals of **L** and compounds **1**–**3** were mounted on a Rigaku Mercury CCD diffractometer equipped with a graphite-monochromated Mo-K_α radiation (λ = 0.71073 Å) at 298 K. The CrystalClear software package was used for data reduction and empirical absorption correction.[29] Empirical absorption corrections were performed using the SADABS program.[30] All structures were solved by direct methods and refined by full-matrix least-squares fitting on F^2 by SHELXTL-97.[31] All non-hydrogen atoms were refined with anisotropic thermal parameters. Hydrogen atoms were located at geometrically calculated positions and treated as in riding mode. Crystallographic data and structural refinements for **L** and compounds **1**–**3** are summarized in Table 2. Selected bond lengths and angles are listed in Table 3.

CCDC-703993 (for **L**), 703994 (for **1**), 703995 (for **2**), and 703996 (for **3**) contain the supplementary crystallographic data for this paper. These data can be obtained free of charge from The Cambridge Crystallographic Data Centre via www.ccdc.cam.ac.uk/data_request/cif.

Acknowledgments

This work was supported by the National Science Foundation of China (20773129, 21003125, 21073190), the 973 Program (2006CB932903), and the National Science Foundation of Fujian Province (2010J05040, 2010J01057).

[1] M. J. Zaworotko, *Angew. Chem. Int. Ed.* **2000**, *39*, 3052–3054.
[2] V. A. Russell, C. C. Evans, W. J. Li, M. D. Ward, *Science* **1997**, *27*, 6575–579.
[3] M. Fujita, D. Oguro, M. Miyazawa, H. Oka, K. Yamaguchi, K. Ogura, *Nature (London)* **1995**, *378*, 469–471.
[4] J. J. Perry IV, J. A. Perman, M. J. Zaworotko, *Chem. Soc. Rev.* **2009**, *38*, 1400–1417.
[5] O. Kahn, C. J. Martinez, *Science* **1998**, *279*, 44–48.
[6] J.-P. Zhang, X.-C. Huang, X.-M. Chen, *Chem. Soc. Rev.* **2009**, *38*, 2385–2396.
[7] W. B. Lin, O. R. Evans, R. G. Xiong, Z. Y. Wang, *J. Am. Chem. Soc.* **1998**, *120*, 13272–13273.
[8] O. R. Evans, W. Lin, *Acc. Chem. Res.* **2002**, *35*, 511–522.
[9] Y. Cui, H.-J. Mo, J.-C. Chen, Y.-L. Niu, Y.-R. Zhang, K.-C. Zheng, B.-H. Ye, *Inorg. Chem.* **2007**, *46*, 6427–6436.
[10] S. Fortin, A. L. Beauchamp, *Inorg. Chem.* **2000**, *39*, 4886–4893.
[11] S. W. Kaiser, R. B. Saillant, P. G. Rasmussen, *J. Am. Chem. Soc.* **1975**, *97*, 425–426.
[12] M. P. Garcia, A. M. López, M. A. Esteruelas, F. J. Lahoz, L. A. Oro, *J. Chem. Soc., Chem. Commun.* **1988**, 793–809.
[13] B. J. Holliday, Ch. A. Mirkin, *Angew. Chem. Int. Ed.* **2001**, *40*, 2023–2043.
[14] J.-S. Casas, A. Castineiras, Y. Parajo, M.-L. Perez-Paralle, A. Sanchez, A. Sanchez-Gonzalez, J. Sordo, *Polyhedron* **2003**, *22*, 1113–1121.
[15] M. Tadomoro, K. Nakasuji, *Coord. Chem. Rev.* **2000**, *198*, 205–218.
[16] M. Tadokoro, K. Isober, H. Uekusa, Y. Ohashi, J. Toyoda, K. Tashiro, K. Nakasuji, *Angew. Chem. Int. Ed.* **1999**, *38*, 95–98.
[17] L. Ohrstrom, K. Larsson, S. Borg, S. T. Norberg, *Chem. Eur. J.* **2001**, *7*, 4805–4810.
[18] R.-L. Sang, L. Xu, *Eur. J. Inorg. Chem.* **2006**, 1260–1267.
[19] R.-L. Sang, L. Xu, *Inorg. Chem.* **2005**, *44*, 3731–3737.
[20] R.-L. Sang, L. Xu, *Inorg. Chim. Acta* **2006**, *359*, 2337–2342.
[21] R. C. Mehrotra, R. Bohra, *Metal Carboxylates*, Academic Press, London, **1983**.
[22] F. A. Cotton, R. H. Walton, *Multiple Bonds between Metal Atoms*, Oxford University Press, Oxford, **1993**.
[23] R. L. Sang, L. Xu, *Chem. Commun.* **2008**, 6143–6145.
[24] P. C. Ford, A. Vogler, *Acc. Chem. Res.* **1993**, *26*, 220–226.
[25] C. M. Che, S. W. Lai, *Coord. Chem. Rev.* **2005**, *249*, 1296–1309.
[26] M. D. Allendorf, C. A. Bauer, R. K. Bhakta, R. J. T. Houk, *Coord. Chem. Rev.* **2009**, *38*, 1330–1352.
[27] Q.-Y. Liu, Y.-L. Wang, L. Xu, *Eur. J. Inorg. Chem.* **2006**, 4843–4851.
[28] W. M. Barnett, R. G. Baughman, H. L. Collier, W. G. Vizuete, *J. Chem. Crystallogr.* **1999**, *29*, 765–768.
[29] CrystalClear version 1.3, Rigaku Corp., **2000**.
[30] G. M. Sheldrick, *A program for the Siemens Area Detector Absorption correction*, University of Göttingen, **1997**.
[31] G. M. Sheldrick, *SHELXS 97*, Program for Crystal Structure Solution, University of Göttingen, **1997**.

Received: April 22, 2010
Published Online: September 23, 2010

